Nonlinear Behavior of a Suspended Particle in Single-Axis Acoustic Levitators

C. V. Abud
Institute of Mathematics and Technology.
Federal University of Goiás - UFG, Goiás, Brazil.

M. S. Rodrigues
Department of Mining Engineering,
Federal University of Goiás - UFG, Goiás, Brazil

T. S. Ramos
Department of Mechatronics and Mechanical Systems Engineering,
University of São Paulo - USP, São Paulo, Brazil

Abstract

The nonlinear behavior of a suspended sphere in a single-axis acoustic levitator was studied. Spontaneous oscillations of the sphere in this levitator were experimentally analyzed recording its positions using a high speed camera. A mathematical model based on acoustic radiation forces and real parameters is proposed to describe the dynamics of the sphere movement and its stability. The stability of the motion was investigated via a Lyapunov exponent diagram. We observed that the axial and radial movements of small spheres under levitation may present regular stability and chaotic ones. The Lyapunov exponent diagram for the model shows a complexity structure sharing different regions of stability according to the model parameters.

Keywords: Nonlinear Phenomena; Acoustic Levitation; Lyapunov Exponents.

1. Introduction

Acoustic levitation has emerged as a powerful technique for contactless processing of materials. Due to its property of being material independent, the acoustic handling technique has been used in a wide range of areas including pharmaceutical processes[1], biology[2], manipulation of microcomponents[3], separating lipids in blood[4], analytical chemistry studies[5], Ramam spectroscopy in red blood cells[6] and scattering of nanoparticles[7], among others.

New acoustic devices have been developed to levitate and also manipulate small objects. In particular, the most common type of acoustic levitator, called single-axis[8], consists of producing a standing wave field in the air gap between an ultrasonic transducer and a reflector separated by a

multiple integer number of a half wavelength. In such a device, samples much smaller than the wavelength may be levitated by acoustic radiation forces, which push the particle towards a pressure node. At the pressure nodes, it has a minimum acoustic potential energy and the levitation force is zero, generating an equilibrium position (see Fig. 1). Everywhere else between the reflector and transducer, levitation forces act in the direction of the nearest node, and therefore the equilibrium of pressure nodes may counteract the gravity force. Indeed, the equilibrium position is slightly displaced from the minimum energy potential due to gravity force.

Recent studies have related that samples in acoustic levitation do not remain static but oscillate in a particular trajectory around the equilibrium point[9,10]. Under low pressure amplitudes, usually located near the transducer or reflector in a single - axis levitator, the experimental results show that sphere oscillations can be described by the simple spring- mass system [9]. However, this model cannot be applied for samples levitating at the central node, because of prominent nonlinear effects in this region.

In the present paper, we are interested in investigating the nonlinear effects of acoustic radiation forces in the trajectories described by a small sphere levitating at the central node position. The trajectories in horizontal and vertical directions are obtained through a mathematical model and compared to experimental data. In addition, a stability diagram based on Lyapunov exponents is investigated and the results point to a complex frontier between chaotic and periodic motions.

The paper is organized as follows. Section 2 describes the theoretical determination of radial and axial radiation force. In Section 3, we introduced some analysis into the experimental data. The results based on an analytical model for the radial (horizontal) and axial (vertical) movement of a suspended small sphere are presented in Section 4. Some numerical analysis are proposed in Sec.5. Finally, we conclude our investigations in Section 6.

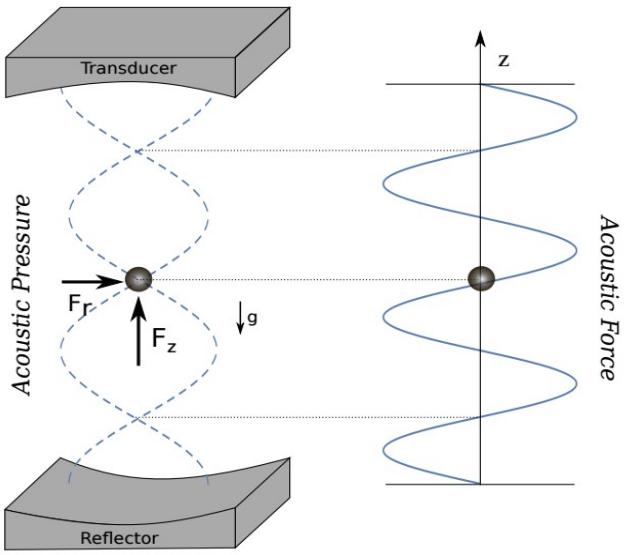

Figure 1: Axial radiation force, F_z , and radial radiation force, F_r , acting on a small sphere in a single-axis levitator.

2. Fundamental Forces

In the acoustic levitation process of a single-axis levitator, basically two radiation forces act on a single object. The primary radiation force in the axial direction, F_z, acts in the direction of propagation of the wave and is the responsible for counteracting the gravity force. The second force is a transversal component denoted as radial radiation force, F_r. This component is two orders of magnitude smaller than the axial component and arises due to diffraction effects of the transducer energy field, as well as the geometric imperfections of the reflector. Forces F_z and F_r acting on a small sphere in an acoustic levitator are illustrated in Fig. 1.

Now, let us revisit the theory of radiation forces that act in a single sphere in acoustic levitation from an acoustic pressure field in a cylindrical levitator assumed as the standing wave,

$$P(r,z,t) = P(r)\cos(kz)\cos(\omega t), \tag{1}$$

where k is the wavenumber, and ω is the angular frequency of the wave. The acoustic pressure amplitude, $P(r)$, which varies with the radial position, is assumed as a zero-order Bessel function[11,12].

According to Gor'kov [13], the acoustic force on a spherical small particle is given by:

$$F = VB\nabla\langle KE\rangle - V_s(1-\beta_p/\beta_m)\nabla\langle PE\rangle, \tag{2}$$

where: V is the particle volume; β_p and β_m are the adiabatic compressibility of the particle and host medium, respectively. $\langle KE\rangle$ and $\langle PE\rangle$ are the temporal-average kinetic and potential energy densities of the acoustic field, respectively. Quantity B results from the relative motion between the particle and the surrounding fluid. It is defined for spherical particle very small when compared to the wavelength as, $\mathrm{B}=3(\rho_p-\rho_m)/(2\rho_p+\rho_m)$, where ρ_p and ρ_m are the densities of the particle and the medium, respectively.

The temporal average potential density $\langle PE\rangle$ is defined by,

$$\langle PE\rangle = P^2(r)\beta cos^2[kz]/4, \tag{3}$$

where we used the relation to the acoustic pressure, $\langle PE\rangle = \langle P^2(r,z,t)\beta_m/2\rangle$.

Otherwise, the kinetic energy density $\langle KE\rangle$ is given by

$$\langle KE\rangle = P^2(r)\beta_m/4 - \langle PE\rangle, \tag{4}$$

obtained by assuming the approximation, $\nabla P(r,z,t) = [\partial P(r,z,t)/\partial z]\hat{z}$ and also the relation to the acoustic pressure, $\langle KE\rangle = \langle\left[\int \nabla P(r,z,t)dt\right]^2/2\rho_m\rangle$.

Therefore, the axial component F_z can be obtained by Eq. (2) combined with Eq. (3) and (4),

$$F_z = VP^2(r)\left[B + \left(1 - \frac{\beta_p}{\beta_m}\right)\right]\left[\frac{k}{4}\right]\sin[2kz]. \quad (5)$$

The axial radiation force is the primary force due to the interaction between the particle and the wave field. As the axial force acts in the normal direction to the propagation of the acoustic wave, its magnitude can balance the force of gravity, and therefore levitation of the particle is possible. It is important to note that Eq. (5) is in accordance with the theory developed by Yosioka and Kawasima[14].

Also according to Eq. (2), the radial force component is given by,

$$F_r = \frac{V}{4}\left[\frac{\partial P^2(r)}{\partial r}\right]\left\{B - \left[B + \left(1 - \frac{\beta_p}{\beta_m}\right)\right] cos^2\,[kz]\right\}. \quad (6)$$

The axial and radial radiation forces are fundamental forces for the stability of the particle in a levitation process. In the next section, we will show experimental data for the movement in radial and axial directions of a suspended particle in a single - axis levitator.

3. The Experimental data

The data set used in this paper was obtained by a single-axis acoustic levitator of a 20.3 kHz Langevin type transducer and reflector. Both, the transducer and reflector have a concave radiating surface with a curvature radius of $35mm$ and $33mm$, respectively. The complete description of this levitator can be seen in Ref. [15].

In order to determine the displacement of a small sphere in levitation in relation to the equilibrium position, an image evaluation technique is proposed. The motion of the sphere is recorded by a high-speed camera, then the displacement to the center is obtained by an algorithm that returns, for each frame of the camera, the positions (x, z). Thus, a time series is obtained for the horizontal and vertical movement. Figure 2 shows a time series of positions for both x and z - direction of a $4mm$ diameter glass sphere. In addition we calculated the frequencies of the particle oscillation using Fast Fourier Transform (FFT). The FFT of the sphere oscillations in the x and z directions are shown, respectively, in Fig. 2 (B) and (D).

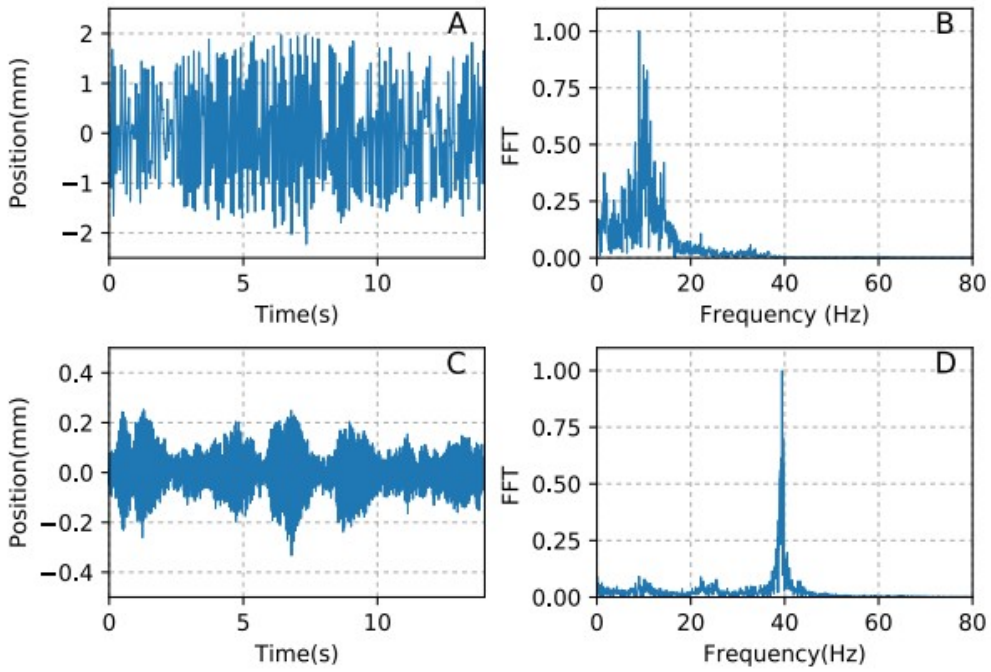

Figure 2: (A) and (C) - Time series of the horizontal and vertical movement, respectively, of glass sphere in acoustic levitation. Figure (B) and (D) show the fast fourier transform of time series.

In Fig. 2 some particularities of each movement can be observed.. The frequency of oscillation in the z - direction is higher than the horizontal one. On the other hand, the x - direction has higher amplitudes. Indeed, this amplitude variation in the x - direction is attributed to the axisymmetric geometry of the acoustic levitator. From FFT we note that the x - direction presents a well defined peak at approximately 40 Hz and for the z - direction there is no dominant frequency. It is important to stress that horizontal and vertical motion are analyzed separately but the sphere oscillates in both x and z directions at the same time.

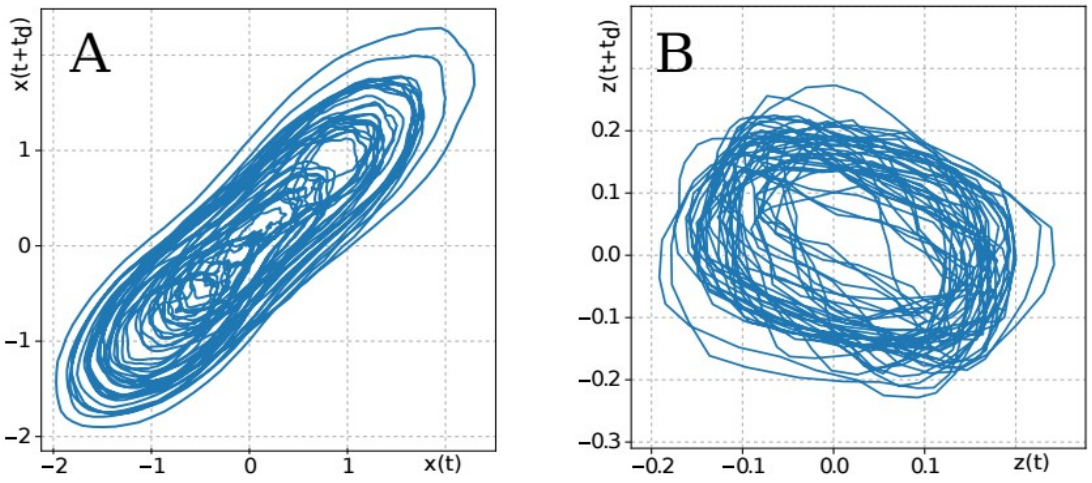

Figure 3: Attractor reconstruction of time series showed in Fig. 2 (A) and (C).

We also constructed the phase plane for both directions $x(t)$ and $z(t)$. Assum$x(t) \times x(t + t_d)$ing an arbitrarily time-delay t_d in the time series, the phase plane is obtained in a $x(t)$ variable plotting: . When

applied to dissipative systems, this technique is called attractor reconstruction

16 In panels (A) and (B) of Fig. 3, the attractor reconstruction is shown for the time series (A) and (C) of Fig. 2. The trajectory in the z-direction seems to spin around a stable focus at $(0,0)$, while the trajectory described in the x-direction move in an irregular way, preferably visiting the points $(1,1)$ and $(-1,-1)$. From a topological point of view, the attractor of Fig.3 (B) (z-direction) is similar to the attractors reported in the literature whose behavior is regular. On the other hand, Fig.3 (A) (x-direction) seems to be a chaotic attractor. To investigate the possible attractors that small spheres in the levitation process may be subject to, we develop a theoretical model based on acoustic radiation forces in the following section.

Table 1. Experimental values for

Parameters	Value	Unit
Diameter of the glass sphere	$4{\cdot}10^{-3}$	m
Glass density	4.540	Kg/m^3
Air density	$1,204$	Kg/m^3
Compressibility of the particle	$1{,}86{\cdot}10^{-11}$	Pa^{-1}
Compressibility of the air	$7{,}06{\cdot}10^{-6}$	Pa^{-1}
Air viscosity	$1{,}80{\cdot}10^{-5}$	$Pa.s$

4. Mathematical Model

Our main aim is to determine the dynamic of the trajectories of a suspended particle in a single-axis levitator. Newton´s second law applied in the axial direction gives:

$$m\frac{d^2z}{dt^2} + 6\pi\mu a\frac{dz}{dt} - VP^2(r)\left[B + \left(1 - \frac{\beta_p}{\beta_m}\right)\right]\left[\frac{k}{4}\right]\sin[2kz] + mg = 0, \tag{7}$$

where the quantity $6\pi\mu a\dot{z}$ is the Stokes' drag force on a small sphere of radius a.

Considering the Taylor series expansion for $sin(2kz)$ at $z = 0$ until the first nonlinear term, and introducing an external periodic force, the Eq. (7) is re-written as,

$$\frac{d^2z}{dt^2} + C_z\frac{dz}{dt} + \gamma_z\left(-z + \frac{2k}{3}z^3\right) + g = D_z\cos(\omega_z t), \tag{8}$$

where, $C_z = 6\pi\mu a/m$ and $\gamma_z = VP^2(r)\left[B + \left(1 - \frac{\beta_p}{\beta_m}\right)\right]\left[\frac{k^2}{2}\right]$.

Using an adimensional time $\tau = \omega_z t$, Eq. (8) is replaced by,

$$\frac{d^2z}{d\tau^2} + \hat{C}_z\frac{dz}{dt} + \hat{\gamma}_z\left(-z + \frac{2k}{3}z^3\right) + g = \hat{D}_z\cos(\tau), \tag{9}$$

where, $\widehat{C}_z = C_z/\omega_z$ and $\widehat{\gamma_z} = \gamma_z/\omega_z^2$.

Thus, Eq. (9) gives the movement of the suspended particle in the axial direction.

Newton´s second law in the radial direction gives:

$$m\frac{d^2x}{dt^2} + 6\pi\mu a\frac{dx}{dt} - \frac{V}{4}\left[B - \left[B + \left(1 - \frac{\beta_p}{\beta_m}\right)\right]\cos^2(kz)\right]\left(\frac{\partial P^2(r)}{\partial r}\right) = 0, \tag{10}$$

Now, let us consider some approximations. Firstly, since the range of movement of the particle in the radial direction is small, we assume $cos(kz) \approx 1$. Furthermore, we consider the Bessel Function $P(r) = P(x) \approx (1 - x^2/4)$. The motivation for such a choice is quite simple. Observe that Eq. (6) can be seen as a resultant of the formula, $F = -\nabla\phi$, where ϕ is the acoustic potential. Choosing $P(x)$ as a truncated Bessel function ($P(x) = 1 - x^2/4$); $P^2(x)$ results in a double well potential, which may determine two preferential regions, in accordance to the characteristic observed experimentally in panel (A) of Fig. 3.

Therefore, re-writing Eq. (10) and considering an external periodic force we have,

$$\frac{d^2x}{dt^2} + C_x\frac{dx}{dt} + \gamma_x\left(-x + \frac{1}{4}x^3\right) = D_x\cos(\omega_x t), \tag{11}$$

where, $C_x = 6\pi\mu a/m$ and $\gamma_x = V(1 - \beta_p/\beta_m)/4m$.

Again, introducing an adimensional time $\tau = \omega_x t$. Therefore, Eq. (11) is replaced by,

$$\frac{d^2x}{d\tau^2} + \widehat{C}_x\frac{dx}{d\tau} + \widehat{\gamma}_x\left(-x + \frac{1}{4}x^3\right) = \widehat{D}_x\cos(\tau), \tag{12}$$

where, $\widehat{C}_x = C_x/\omega_x$ and $\widehat{\gamma}_x = \gamma_x/\omega_x^2$.

Equation (12) gives the movement of the suspended sphere in the radial direction.

It is worth noting that Eq. (9) and Eq. (12) are equivalent equations. i.e., both equations have their nonlinear nature given by a cubic term, which is characteristic of Duffing equations.

4. Numerical Analysis

The numerical procedure to solve Eq. (9) and (12) was obtained by Runge - Kutta with a time step of size $h = 5 \times 10^{-3}$. To compare it with the experiment, we used as a guide the data presented in Table 1, which gives the properties of the sample and the medium considered in this research. In Fig. 4 (A) and (C) we show a typical solution to Eq. (9) ($\widehat{\gamma}_z = 1$, $\widehat{D}_z = 0.125$ and $\widehat{C}_z = 3 \times 10^{-4}$) and Eq. (12) ($\widehat{\gamma}_x = 1$, $\widehat{D}_x = 0.86$ and $\widehat{C}_x = 0.324$), respectively. The attractor of both series is reconstructed in Fig. 4 (B) and

(D) using the time delay $\tau_d = 1.2$.

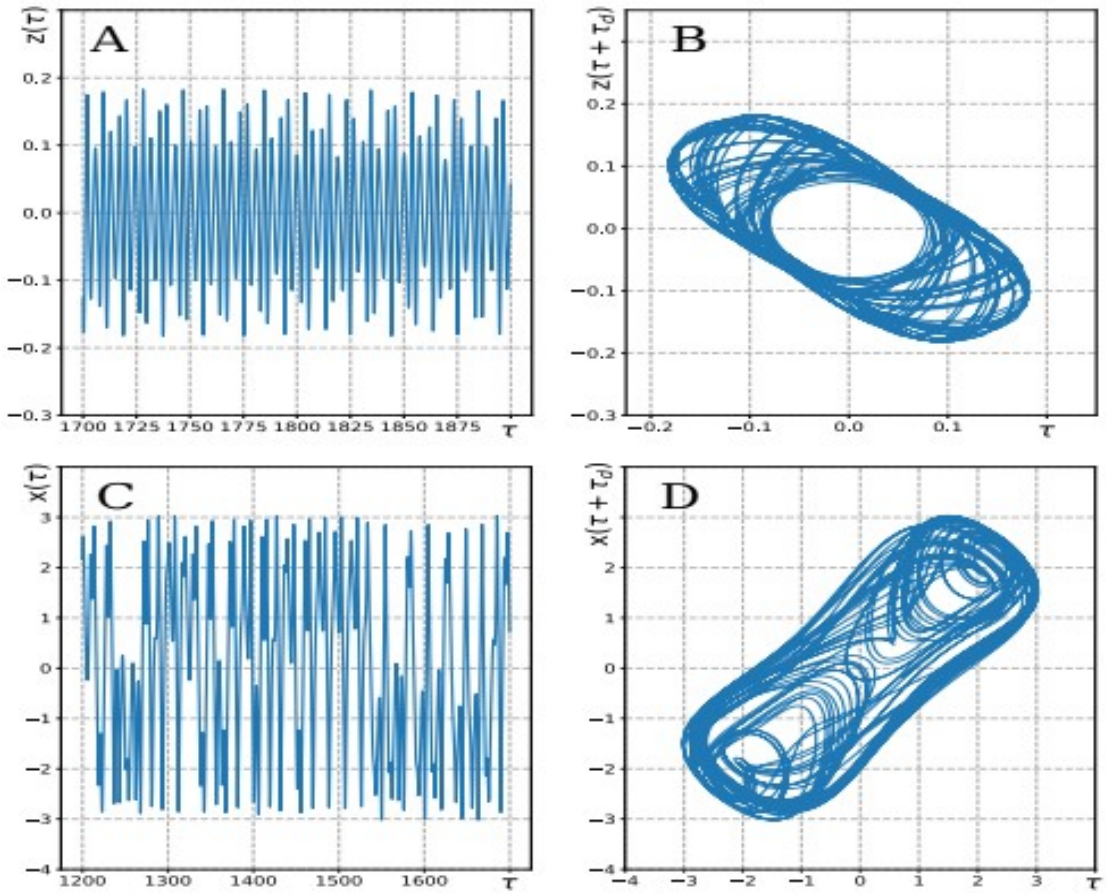

Figure 4: (A) and (C) Part of numerical solution to Eq. (9) ($\widehat{\gamma}_z = 1$, $\widehat{D}_z = 0.125$ and $\widehat{C}_z = 3 \times 10^{-4}$) and Eq. (12) ($\widehat{\gamma}_x = 1$, $\widehat{D}_x = 0.86$ and $\widehat{C}_x = 0.324$), respectively. *(B) and (D) Attractor reconstructed withv* $\tau_d = 1.2$.

Comparing the analytical attractor of Figs. 4 (B) and (D) to their respective experimental attractor of Fig. 3, we observed a good topological agreement. Therefore, a question arises naturally: if Eq. (9) and Eq. (12) describe the vertical and horizontal movement of suspended particles, what kind of behavior can the trajectories assume? And how are the set of parameters related to such behavior?

Both questions can be evaluated by calculating the Lyapunov exponents onto the space of the parameters. Such Lyapunov exponents are standard measures used to discriminate between chaos and periodicity and, the projection of Lyapunov exponents onto the space of the parameters is called Lyapunov diagrams[17–19].

To evaluate the Lyapunov diagram for Eq. (12) we fixed $\widehat{\gamma} = 1$ and we divided the space parameter $(\widehat{C}_x, \widehat{D}_x)$ into a grid of 800×800. In our simulation, for each point $(\widehat{C}_x, \widehat{D}_x)$ of Eq. (12) we computed the Lyapunov exponent according to the method described in Ref. [20], starting a fixed arbitrarily initial condition. We discarded the first 10^5 time-steps to reach the final attractor. Finally, each value for the Lyapunov exponent related to the point $(\widehat{C}_x, \widehat{D}_x)$ was displayed in a palette of colors as shown in Fig. 5.

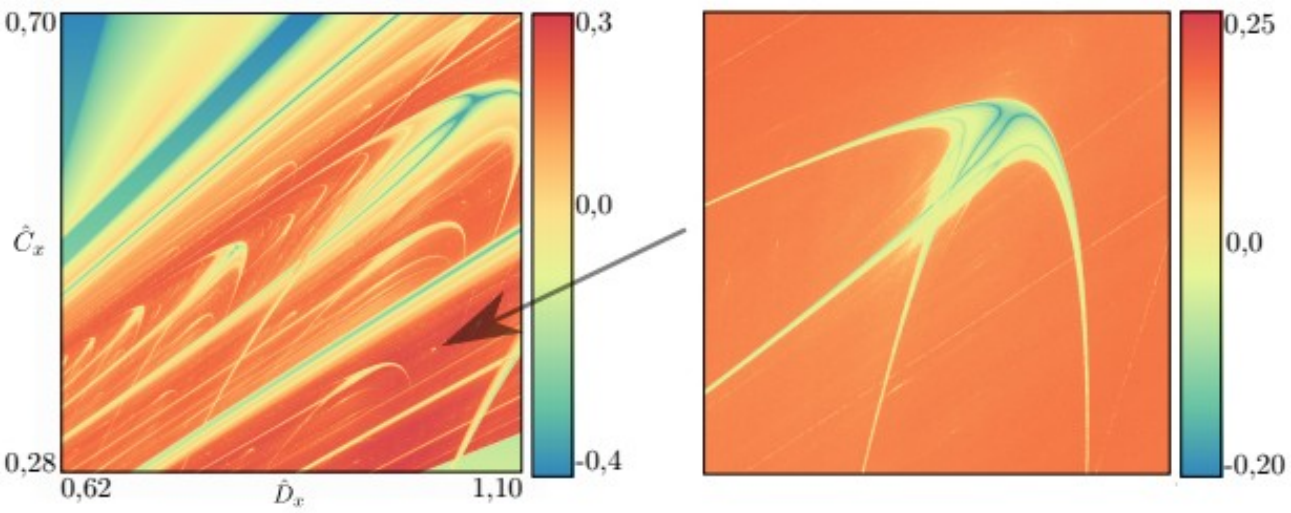

Figure 5: Lyapunov diagram of Eq.(12) for a grid of 800×800. *Lyapunov exponents are posed in colors according to the pallete. The picture at right emphasizes a periodic window in a finer scale with* $\widehat{C}_x \in [0.38605 : 0.39655]$ *and* $\widehat{D}_x \in [1.001; 1.0136]$.

In Fig. 5 it can be observed that the horizontal trajectories of a suspended particle may assume periodic ($\gamma < 0$), quasi-periodic ($\gamma = 0$) and chaotic behavior ($\gamma > 0$) according to the complexity structures presented in the diagram. In particular, we observe in Fig. 5 that the set parameters, whose solutions of Eq.(12) behave periodically, are in aggregated periodic windows (yellow area) also known as shrimps [17]. Such structures present a complex frontiers between chaotic and periodic motions and may exist in different scales as emphasized in the amplification of the figure.

We stress that the same structures are expected for the axial movement since Eq. (9) is very similar to Eq. (12).

4. Conclusions

This paper presented the nonlinear characterization of trajectories described by a small sphere in a single-axis acoustic levitator. The trajectories were obtained experimentally by image treatment and also modeled using the acoustic radiation force theory. The time series generated by experimental data showed typical topologies of nonlinear systems, as a chaotic attractor in the horizontal movement. Such behavior was confirmed qualitatively by a mathematical model and numerical simulations. It was observed that the existence of chaotic attractors related to the horizontal/vertical movement depends on an external force and its stability is linked to a complex diagram full of periodic windows (regular zones) and chaos. The study of how the nonlinear acoustic forces affects the particle stability (Lyapunov diagram) may help to comprehend how to minimize the amplitudes of the spontaneous oscillations. We believe that the experimental and numerical concept presented in this paper are important to understand the fundamentals of successful acoustic levitation: sufficient levitation force and stability.

Regarding future studies, two different strategies can be adopted to take into account the amplitude of spontaneous oscillations in a mathematical model. The first is related to the fact that such oscillations are due to a time delay between the change of the object position and the acoustic radiation force acting on the particle. The second modification includes instabilities of the second harmonic. When the levitator operates with high pressure amplitudes, part of the energy is transferred from the fundamental frequency to its harmonics, which can change the sound pressure distribution and the acoustic radiation force that acts on the particle.

6. Acknowledgement

The authors would like to thank the Brazilian agencies: CAPES/FAPEG (88881.127849/2016-01) and CNPq (458805/2014-9) for the financial support.

6. References

[1] R. J. K. Weber, C. J. Benmore, S. K. Tumber, A. N. Tailor, L. S. T. C. A. Rey, S. R. Byrn, Acoustic levitation: recent developments and emerging opportunities in biomaterials research, Eur. Biophys. J. 41 (2012) 379.

[2] A. Scheeline, R. L. Behrens, Potential of levitated drops to serve as microreactors for biophysical measurements, Biophys. Chem. 165-166 (2012) 1.

[3] C. R. P. Courtney, C. E. M. Demore, A. G. H. Wu, P. D. W. S. Cochran, B. W. Drinkwater, Independent trapping and manipulation of microparticles using dexterous acoustic tweezers, Appl. Phys. Lett. 104 (2014) 154103.

[4] F. Petersson, A. Nilsson, C. Holm, H. J ̈onsson, T. Laurell, Separation of lipids from blood utilizing ultrasonic standing waves in microfluidic channels, Analyst 129 (2004) 938.

[5] S. Santesson, S. Nilsson, Airborne chemistry: Acoustic levitation in chemical analysis, Anal. Bioanal. Chem. 378 (2004) 1704.

[6] L. Puskar, R. Tuckermann, T. Frosch, J. Popp, V. Ly, D. McNaughton, B. R. Wood, Raman acoustic levitation spectroscopy of red blood cells and plasmodium falciparum trophozoites, Lab Chip 7 (2007) 11251131.

[7] J. Schenk, L. Trobs, F. Emmerling, J. Kneipp, U. Panne, M. Albrecht, Simultaneous uv/vis spectroscopy and surface enhanced raman scattering of nanoparticle formation and aggregation in levitated droplets, Anal. Methods 4 (2012) 12521258.

[8] W. J. Xie, B. Wei, Parametric study of single-axis acoustic levitation, Appl.Phys. Lett. 79 (2001) 881883.

[9] M. A. B. Andrade, N. Péres, J. C. Adamowski, Experimental study of the oscillation of spheres in an acoustic levitator, J. Acoust. Soc. Am 136 (2014) 1518.

[10] N. Péres, M. A. B. Andrade, R. Canetti, J. C. Adamowski, Experimental determination of the dynamics of an acoustically levitated sphere, Journal of Applied Physics 116 (2014) 184903.

[11] G. Whitworth, M. A. Grundy, W. T. Coakley, Transport and harvesting of suspended particles using modulated ultrasound, Ultrasonics 29 (1991) 439.

[12] G. Whitworth, W. T. Coakley, Particle column formation in a stationary ultrasonic field, J. Acoust. Soc. Am. 91(1) (1992) 79.

[13] L. P. Gor'kov, On the forces acting on a small particle in an acoustic field in an ideal fluid, Sov. Phys. Doklady 6 (1962) 773.

[14] K. Yosioka, Y. Kawasima, Acoustic radiation pressure on a compressible sphere, Acoustics 5 (1955) 167.

[15] M. A. B. Andrade, T. S. Ramos, F. T. A. Okina, J. C. Adamowski, Nonlinear characterization of a single-axis acoustic levitator, Rev. Sci. Instrum. 85 (2014) 045125.

[16] F. Takens, Detecting strange atractors in turbulence, Lecture Notes in Mathematics 898 (1981) 366.

[17] J. Gallas, Structure of the parameter space of the Hénon map, Phys. Rev. Lett. 70 (1993) 271.

[18] E. Medeiros, S. de Souza, R. Medrano, I. Caldas, Replicate periodic windows in the parameter space of driven oscillators, Chaos, Solitons & Fractals 44 (2011) 982 – 989.

[19] C. V. Abud, R. E. de Carvalho, Robust attractor of non-twist systems, Physica A 440 (2015) 42.

[20] J. C. Sprott, Chaos and time-series analysis, Oxford University Press 91(1) (2003) 116–117.